



# Empirical assessment of rockfall and debris flow risk along the Karakoram Highway, Pakistan

Sajid Ali<sup>1,2</sup> · Rashid Haider<sup>3,4</sup> · Wahid Abbas<sup>1,2</sup> · Muhammad Basharat<sup>5</sup> · Klaus Reicherter<sup>1</sup>

Received: 21 October 2019 / Accepted: 19 January 2021 / Published online: 15 February 2021  
© The Author(s) 2021

## Abstract

The Karakoram Highway links north Pakistan with southwest China. It passes through unique geomorphological, geological and tectonic setting. This study focused 200-km-long section of the highway starting from Besham until Chilas. Landslides are frequent and are mostly triggered by torrential rain during Monsoon and Westerlies, leading to highway blockade. Rockfall and debris flow are prime mode of slope failures. Regional to site-specific approach was implemented to assess risk associated with these two modes. Remote sensing-based techniques were used to identify potential hazardous sites, which were further investigated for risk assessment. Modified Pierson's rockfall hazard rating system (RHRS) rated potential rockfalls, whereas semi-quantitative technique was employed to assess debris flows. Normalized scores of each site shaped the final map, further classified into four zones: very high, high, intermediate and low risk.

**Keywords** Risk assessment · Landslide · Rockfall · Debris flow · Karakoram Highway

## 1 Introduction

The Karakoram Highway (KKH) is a lifeline of North Pakistan, more specifically of the Gilgit Baltistan. It is also an important trade route between Pakistan and China (Fig. 1a). It passes through one of the most challenging and rugged terrains of the world. Stability of the 840-km-long KKH is in question since its completion in 1979 (Ali et al. 2018b). Its construction by aggressive uncontrolled blasting resulted into large number of landslides.

---

✉ Sajid Ali  
s.ali@nug.rwth-aachen.de

<sup>1</sup> Neotectonics and Natural Hazards, RWTH Aachen University, Lochnerstr. 4–20, 52056 Aachen, Germany

<sup>2</sup> Department of Earth Sciences, COMSATS University Islamabad, Islamabad, Pakistan

<sup>3</sup> Institut of Geosciences-Geology, Rheinische Friedrich-Wilhelms-Universität Bonn, 53115 Bonn, Germany

<sup>4</sup> Geological Survey of Pakistan, Islamabad, Pakistan

<sup>5</sup> Institute of Geology, University of Azad Jammu and Kashmir, Muzaffarabad, Pakistan

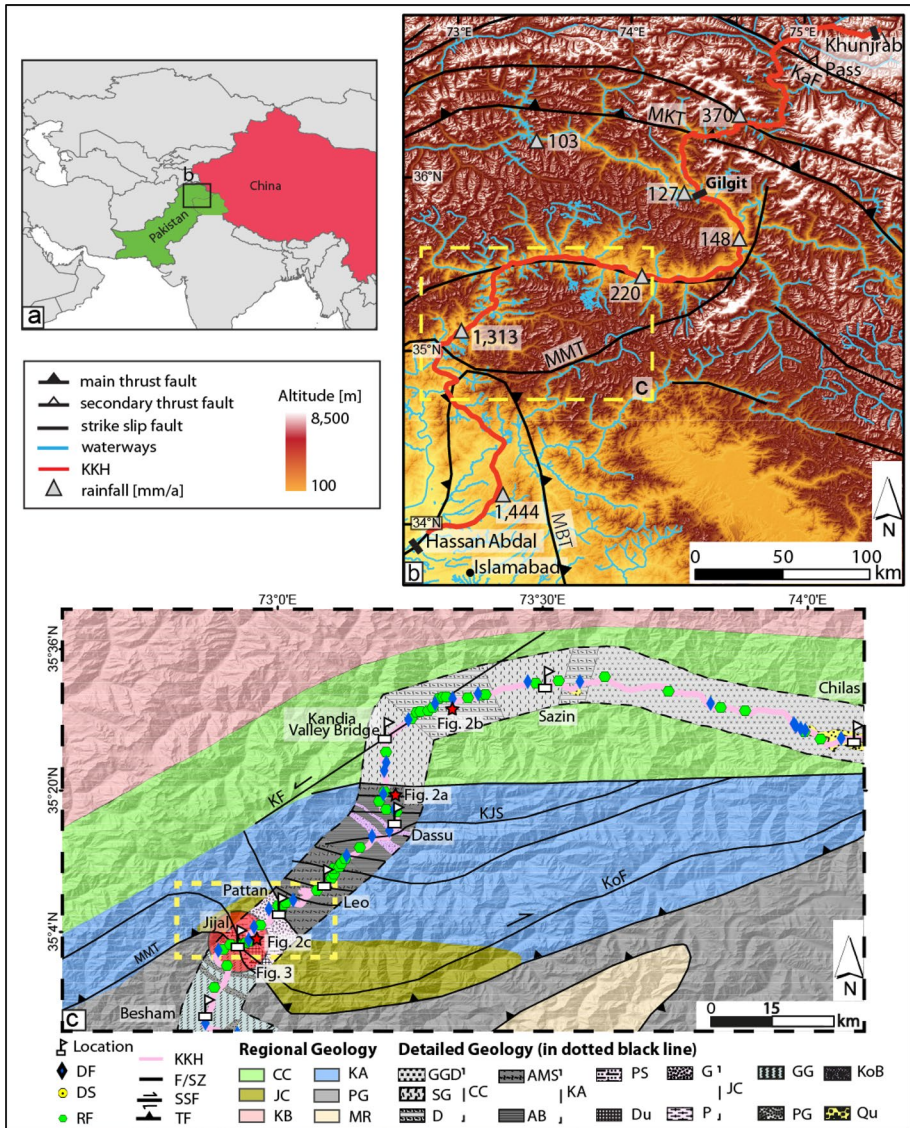


**Fig. 1** Overview of study area **a** location of the study area, **b** overview of weather conditions and tectonics, **c** geology of the study area: *DF* debris flow, *DS* debris slide, *RF* rockfall, *CC* Chilas complex, *KA* Kamila amphibolite, *JC* Jijal complex, *GGD* gabronorite, gabbro and diorite, *D* diorite, *SG* sheared gabronorite, *AB* amphibolite banded, *AMS* sheared amphibolite, *G* garnet gabbro, *P* pyroxenite, *Du* dunnite, *PS* pyroxenite and serpentinite, *BG* Besham group, *PG* porphyritic granite, *Q* quaternary, *MMT* Main Mantle Thrust, *KaF* Karkoram fault, *KF* Kamila fault, *KoF* Kohistan fault, *KJS* Kamila-Jal shear zone, *MKT* Main Karkoram Thrust, *MBT* Main Boundary Thrust. Red circles and dotted yellow rectangle show locations of Fig. 3

Variation in geological, seismological and atmospheric environments makes it a unique area to study and investigate landslide hazard. Interruption of traffic along the KKH, due to landslides, during rainy seasons (Monsoon and Westerlies) is a regular phenomenon. Additionally, it results into life losses and economic losses (Fig. 2). Depending upon magnitude



**Fig. 2** Impact of rockfalls and debris flows on traffic and travellers: **a** Rockfall near Dassu crashes cars. Yellow arrows indicate crashed cars (KKH Updates 2016). **b** Debris flow trapped a car along the KKH. **c** Small debris flow blocked the highway for couple of hours, and two yellow lines show long line of vehicles on one side of deposit

of the landslide, traffic blockade may extend to a couple of weeks. On April 2, 2016, due to torrential rainfall, landslides at more than hundred locations blocked the KKH for more than two weeks and killed 16 people (Petley 2016). Furthermore, landslides at Chuchang and Kiyal Bridge completely eroded the highway. Previously, most of the research work along the KKH was regional landslide susceptibility mapping (1:100,000) based on remote sensing techniques (Kamp et al. 2008; Ahmed et al. 2014; Kanwal et al. 2016; Basharat et al. 2016; Bacha et al. 2018; Khan et al. 2018; Rahim et al. 2018). In this paper, an attempt is made to assess risk associated with landslide along 200-km-long Besham-Chilas section of the KKH (Fig. 1). Rockfall, debris slide and debris flow are dominant mode of slope failures in the section.

Risk associated with these processes is defined as the probability of their occurrence and capacity to damage exposed elements (Mineo et al. 2018). Previous researchers used empirical and semi-empirical techniques to evaluate hazard and risk associated with above landslide processes (Capra et al. 2002; Hürlimann et al. 2006; Gentile et al. 2008; Liu et al. 2009; Baumann et al. 2010; Lari et al. 2011; Santi et al. 2011; Wrachien and Mambretti, 2011; Chen et al. 2012; Liang et al. 2012; Cui et al. 2013; Ma et al. 2013; Rickenmann, 2016; Cao et al. 2016). One element is common that all techniques are based on factors responsible for occurrence of landslide and capacity to damage exposed elements. Factors controlling occurrence and its probability are different for each landslide process (rockfall and debris flow). Unique and relevant risk assessment methods are necessary for each landslide process. Therefore, primary knowledge about each failure mode is essential to define, design and implement risk assessment methods.

Extremely rapid downslope movement of a detached block by free fall, rolling, leaping and bouncing is known as rockfall (Varnes 1978). Frequency of rockfall is high along roads and highways, which have been excavated along steep cliffs. The presence of faulted and sheared massive ultramafics, mafics and batholiths made this section highly susceptible to rockfalls.

Previously, event trees (Peila and Guardini, 2008; Budetta et al. 2016; Mineo et al. 2017) and rating approach (Budetta 2004; Ferlisi et al. 2012; Regmi et al. 2016) have been widely used for rockfall risk assessment. Availability of relevant data regarding rockfall events and objective of the study influence the choice of method.

In this case study, the documentation of historical events is very poor and is not enough to determine recurrence of rockfall. Therefore, we did not employ statistical method and use modified rockfall hazard rating system initially developed by Pierson et al. (1993). We used previously developed susceptibility map (Ali et al. 2018a), limited historical landslide inventory, slope angle distribution (SAD) and runout assessment to zoom into potential rockfall sites.

In addition to rockfalls, a large number of debris slides and flows characterize this section of the KKH. Debris slide and flow are two different slope failures, but their progressions have slight commonality (Sletten et al. 2015). The presence of collapsed material in terms of talus, scree or moraine deposits on steep slopes is highly susceptible to erosion. Melting of snow coupled with precipitation triggers debris slides and flows. Initial rise in pore water pressure leads into debris slide, and further upsurge in water content leads into flow of collapsed material into a channel. Sometimes, light rain removes fine particles from collapsed material leaving behind coarser one with low shear strength. Risk assessment of debris slide and flow involves identification of parameters essential for their formation and initiation. Previous researchers used regional approach involving remote sensing, detailed field survey for simulations and statistical analysis of causative factors for risk assessment of debris slide and flows (Capra et al. 2002; Hürlimann et al. 2006; Gentile et al. 2008; Liu et al. 2009; Baumann et al. 2010; Santi et al. 2011; Wrachien and Mambretti, 2011; Lari et al. 2011; Liang et al. 2012; Chen et al. 2012; Cui et al. 2013; Ma et al. 2013; Rickenmann, 2016;). In this study, maximum probability of debris flow was calculated by using pre-defined sources on Flow-R. Afterwards, detailed field survey was conducted to rate indexes responsible for its formation and initiation.

## 2 General situation of the study area

### 2.1 Location and weather conditions

The study area is a section of the KKH, located in North Pakistan (Fig. 1b). It starts from town of Besham and ends at Chilas. The Jijal, Pattan, Dasso and Sazin are important towns located along the section of the highway. It runs through deep gorges and along the Indus River. From Besham onwards, it follows right bank of the river until Dasso where it crosses the river and then runs along left bank. The section is characterized by steep ( $45^{\circ}$ – $80^{\circ}$ ) and long slopes (2–3 km). The study area receives heavy rainfall in two seasons: monsoon and westerlies. However, weather conditions along the section are not uniform. Area in North of Besham until Sazin receives heavy rainfall (1000–1500 mm/y), whereas area in East of Sazin until Chilas lies in semi-arid to arid climate (0–250 mm/y). In April 2016, due to torrential rainfall in March and April (281.8 and 335, respectively) triggered multiple landslides leading to blockage of the KKH for more than two weeks.

## 2.2 Geology, geomorphology, tectonics and seismology

Southern part is located at northern part of Indian plate, whereas northern is situated at central part of Kohistan Island Arc (KIA). It demonstrates a wide range of lithology, different tectonic environments and seismic zones. It runs through cliff forming granitic gneisses of Indian plate, mafic and ultramafics of KIA. Slopes in study area are composed of thirteen (13) lithological units (Fig. 1c). Four important tectonic features cross or lie in close vicinity of the KKH in this section: Main Mantle Thrust (MMT), Pattan fault (PF), Kamila-Jal shear zone (KJS) and Kamila fault (KF). Rock mass is closely jointed and highly fractured close to these tectonics features. Due to position at hanging wall of MMT, dunnites, pyroxenites and serpentinites of Jijal complex are closely jointed and sheared at places. Therefore, it exhibits a large of number of slope failure. Differential erosion in massive and sheared Kamila amphibolite is responsible for dangerous rockfalls. Gabbro-norites and diorites of Chilas complex contains stress release joints with short persistence leading to block formation of size more than  $6\text{m}^3$  (Ali et al. 2018b). Furthermore, ongoing rockfall process has led to formation huge talus deposits on slopes. These talus deposits are highly susceptible to erosion during heavy rainfall and snowmelt at the start of spring season.

Seismically, the area is part of two active seismic zones: Indus Kohistan Seismic Zone (IKSZ) and Harman Seismic Zone (HSZ) (Ali et al. 2018a). Former comprised of two events (Pattan 1974:  $M=6.2$  and Kashmir Earthquake:  $M=7.6$ ) which severely damaged the highway (Ambraseys et al. 1981). Close to Jijal area, maximum seismic intensity of Pattan Earthquake was VIII with PGA value of 64.3% g (USGS) (Fig. 3). HSZ also contains instrumental seismicity with one major event (1981:  $M=6.2$ ) (USGS).

The studied part of the highway passes through steep sided v-shaped valley. Valley widens at some places (Pattan and Sazin). After Sazin, it narrows down into steep sided v-shaped valley again. Further, it enters into “Chilas Plains” with valley width between 0.5 to 2 km (Kibria and Masud 2006). Slope angle varies between  $40^\circ$  and  $85^\circ$ , depending upon lithology and structural condition of the slope. Sub-vertical to vertical cut slopes and overhangs are important character of the section.

## 3 Identification of potential hazardous sites (regional)

Methodology for hazard and risk assessment of rockfalls and debris flows along the section comprised of two steps: (1) identification of potential slope failures by using regional approach and (2) field surveys to measure all the parameters for hazard and risk assessment. We used previous publications, remote sensing and field data to prepare risk assessment map of the studied section. Regional to site-specific approach was used.

Remote sensing (DEM, satellite optical imagery), previous events-based inventory and empirical model (Flow-R) were employed to identify potential rockfalls and debris flows. Landslide inventory gave an overview of rockfalls and debris flows. Slope angle distribution (SAD) explored rockfall source areas. Satellite imagery was used to map collapsed material for debris flows, and then, Flow-R assessed runout, propagation and probability of both rockfalls and debris flows.

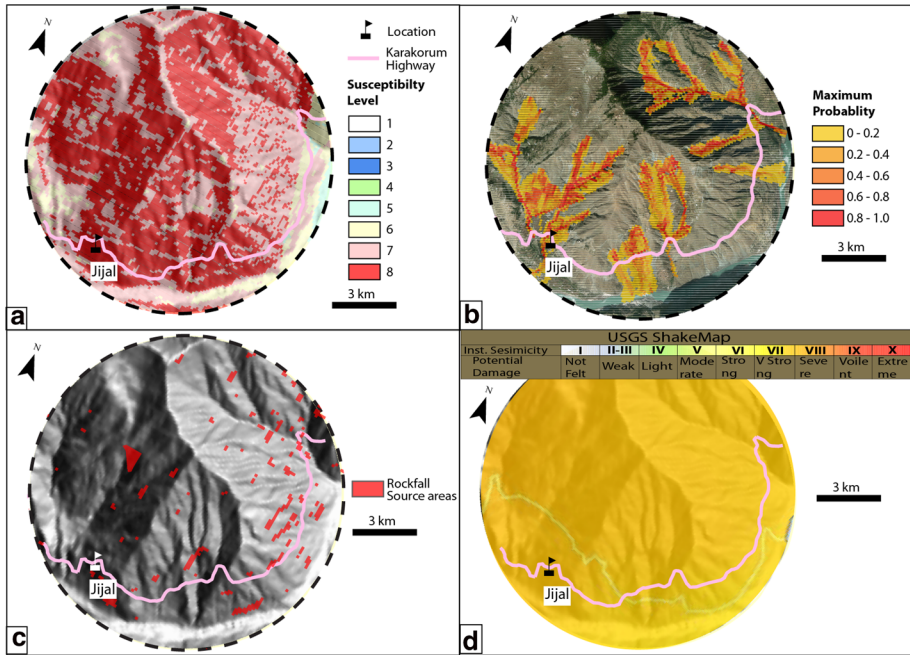


**Fig. 3** Identification of potential rockfalls and debris flows: some parts of the studied section are shown as examples **a** published susceptibility map (Ali et al. 2018a, **b**) Flow-R runoff assessment for debris flows indicating maximum probability along highly active zone, **c** slope angle distribution to extract rockfall source areas, **d** shake map of an previous event (Pattan Earthquake 1974,  $M=6.2$ ) explaining seismic intensity variations along the highway

### 3.1 Landslide inventory

Firstly, multi-temporal, Google Earth 3D images were analysed to mark previous slope failures along the section. Then, published reports (Fayaz et al. 1985; Khan et al. 1986, 2003) and articles (Hewitt 1998, 2001; Derbyshire et al. 2001; Kibria and Masud 2006; Hewitt et al. 2011; Santi et al. 2011) were used to prepare landslide inventory map of the section. Secondly, road clearance data for three different periods (1982–82, 1996–2000, 2014–16) were also supplemented to know about the frequency of landslide events (Fig. 5). Thirdly, field surveys were conducted to validate and complete the landslide inventory map and to further acquire parameters required for risk assessment (Fig. 1c).

### 3.2 Slope angle distribution (SAD)

A morphological unit tends to have several mean slope angles with least standard deviation. Generally, four types of morphological units have commonly been discussed (Oppikofer et al. 2014; Loye et al. 2009): plains, foot slopes, steep slopes and cliffs. Fluvial–glacial deposits constitute plains, marked by low angle. Alluvial, debris flow and landslide deposits compose foot slopes, with slope angle ranging from  $10^\circ$  to  $30^\circ$ . Whereas scree/talus/till covered, slopes are steeper with angle  $30^\circ$ – $50^\circ$ . Cliff is the steepest of all morphological units. Slope angle here corresponds to steeper than  $50^\circ$ . Slope steepness is considered

an important element for rockfall initiation. SAD has been widely used for detection of rockfall source zones. Guzzetti et al. (2010), Toppe, (1987) and Jaboyedoff and Labiouse, (2003) took into account cliffs a rockfall source with steepness more than 45°, 60° and 37°, respectively.

Previously, researchers (Loye et al. 2009; Michoud et al. 2012; Losasso et al. 2016) used DEM for construction of normal distribution of slope angle. Afterwards, it has been decomposed into normal distribution of different topographic units: plains, foot slopes, steep slopes, cliffs, etc. Spatial resolution of DEM has a direct impact on quality of curve. We used 12 m (Tandem-X) and 30 m (ASTER) DEM for construction of slope angle distribution to zoom into steep slope and cliffs. The area studied in this paper has a uniform morphotectonic setting. Therefore, we did not divide it into several parts. Slopes and cliffs with angle more than 55° have been considered a potential rockfall source (Fig. 3c).

### 3.3 Material source of debris flow

The origination of debris flow is sum of three basic requirements: slope, water supply and erodible unconsolidated sediments. The presence of collapsed material in terms of unconsolidated soil, moraines, talus, scree, etc., in the catchment area is a basic essential of debris flow initiation (Cui et al. 2013). Estimation and measurement of the source material have always been challenge for investigators. However, remote sensing has made easy to calculate area of catchment and collapsed material. Still to find exact volume is a difficult and time taking task. Collapse material area was digitized by using Google Earth imagery, which was further used to proportionate it with the total catchment area. Afterwards, the validation process was performed during field excursion. Software-based runout assessment utilized these mapped collapsed material for propagation, probability and extent of debris flows. Ratio between these two mapped parameters was further considered for grading debris flow site in terms of hazard and risk assessment.

### 3.4 Runout assessment

Rockfalls and debris flows are only hazardous when they can reach any sort of infrastructure; in our case, it is the highway. Therefore, runout out assessment has been performed to shortlist potential rockfalls and debris flow with high probability. Flow-R is numerical model based an open-source software, initially developed for runout assessment of debris flows at regional level (Horton et al. 2011; Jaboyedoff et al. 2011; Oppikofer et al. 2014). Afterwards, it has been successfully used for rockfalls, avalanches and other modes of mass movements. Its operation capacity with limited data sets and customization according to local morphotectonic conditions motivated for its usage.

Runout calculation processes involve two steps: source identification and spreading assessment. Identification of source areas can be calculated by software itself either by using different data sets like geological maps, DEM and other derived parameters or by using user-defined sources. In our case, we use user-defined sources for runout assessment. Source areas for rockfalls and debris flows were identified by SAD and mapping of collapsed material, respectively. During identification process, mass of source has not been considered, as it is difficult to calculate its volume for such a big area. Spreading assessment is a combination of two customizable algorithms: flow direction and energy balance responsible for maximum travel distance. Flow direction algorithm determines probability of debris flow direction and distribution from a cell. There is wide range of algorithms:

D8, Dx, p8, Holmgren (Tarboton 1997; Fairfield and Laymarie 1991; Holmgren 1994), but Holmgren's algorithm has been extensively used and has also been preferred in our case. It has ability to be modified from multiple flows to single convergent flow according to local conditions. In the end, areas with high probability are combined. Energy-based algorithms determine travel distance of debris flow or rockfall by considering basic energy of a cell. Due to unidentified mass of whole deposit, whole process relies on unit mass.

Shuttle Radar Topography Mission's digital elevation model (SRTM DEM) and Tandem-x with spatial resolution of 30 m and 12 m have been used for runout assessment. User predefined sources were imported. Flow accumulation threshold was set at 1 ha and distance from stream with buffer of 10 m. Holmgren's exponent was customized at 4. Friction loss function was customized with setting of travel angle at 12° and energy limitation of 10 mps. Slope angle and maximum velocity relationship (Horton et al. 2011) determined debris flow's velocity. Due to variation in slope angle along flow path, mean slope angle was considered. Some of the recent debris flow events in the study area were compared to simulation results with different parameters but earlier discussed were found closer.

## 4 Detailed mapping and risk assessment (site specific)

Potential rockfalls and debris flows, identified during first stage, were surveyed for risk assessment. Due to incomplete information regarding event recurrence, statistical techniques have not been used. Two different empirical methods (for rockfall, debris flow), based on morphological, geological and hydrological criterion were used. Measuring and scoring of some parameters is quite easy, while other's evaluation is difficult and subjective. Exponential scoring criteria has been used to sharply differentiate sites with very high risk, which is ultimate objective of this study.

### 4.1 Rockfall hazard rating system (RHRS)

Several researchers assessed rockfall hazard and risk along highways by using RHRS (Budetta 2004; Pritchard et al. 2005; Guzzetti et al. 2010; Regmi et al. 2016). Eleven parameters, grouped into four categories, were utilized for risk assessment: slope morphology, geology, failed rock characteristics and highway-related factors (Table 1). Slope height indicates potential energy of falling block and determines its runout extent. Effective slope height from source area was measured. We considered number of joint sets, their attitude, spacing, planes and their ultimate effect on block formation and its failure. Scanline surveys were only conducted for the sites, found potential during early stage. Measurements of minimum 60 joints on each site were taken by using different tools (measuring tape, Brunton compass, etc.). In each set, attributes of minimum 20 joints were determined. Furthermore, kinematic analysis was performed to evaluate the effect of joints on slope stability.

Seismicity in close vicinity of the highway is a regular phenomenon. Slopes were rated according to intensity level (MMI), taken from shake maps of instrumental seismic events (USGS database 2019). MMI measures the effects of an earth at a specific site. Block size (volume) and mass of failed rock mass indicate amount of energy and its capacity to damage property. For rockfall history, road clearance logs were acquired from Frontier Works Organization (FWO 2016). Vulnerability, sums vehicle risk and damage to road property comprised of three parameters: distance between road and slope (ditch effectiveness), effective countermeasures and decision sight distance (DSD). Distance between road and



**Table 1** Rockfall hazard rating system (modified after Pierson et al. 1993) for risk assessment

Parameters ▼	3 Points	9 Points	27 Points	81 Points
<i>Hazard</i>				
Slope morphology				
Slope height (m)	<7.62	15.24	22.84	30.48
<i>Geology</i>				
Number of joint sets and their effect on slope	2 sets and less No adverse orientation	3 sets and more No adverse orientation	2 sets and less Adverse orientation exists	3 sets and more Adverse orientation exists
Joint spacing (m)	<0.2	0.2–.5	0.5–1	> 1
Joint planes	Rough	Undulating	Planer	Clay filling
Seismic intensity	<6	6–7	7–8	> 8
<i>Failed rock characteristics</i>				
Size of single block (m <sup>3</sup> )	0–0.25	0.25–0.5	0.5–1	> 1
Rockfall history	Few falls	Occasional falls	Many falls	Constant falls
Failed mass at slope toe	No material	A few	Scattered pile	Well-developed pile
<i>Vulnerability</i>				
Percentage of decision sight distance (%)	80–100	60–80	40–60	<40
Ditch effectiveness	Good catchment	Moderate catchment	Limited catchment	No catchment
Protection measures	Fully effective	Partially effective	Ineffective	No countermeasures

slope can avoid damage and minimize risk by trapping falling rock mass. More the distance is, safer it would be. Highway authorities and planners construct barriers, embankments, meshes, etc., to protect road and vehicles. In this rating criteria, the presence and effectiveness of these protective measures to stop falling mass to reach the highway have also been considered. DSD is an actual distance required to make instantaneous decision, in case of obstacle created by rockfall. It is calculated by using following relationship:

$$\text{PDS} = \left( \frac{\text{ASD}}{\text{DSD}} \right) \times 100 \quad (1)$$

where PSDS is percentage of DSD and ASD is actual sight distance. DSD varies according to maximum speed fixed for that particular highway. In our case, it is 60 km/h and actual sight distance is 160 m.

Sum of score of above explained parameters (Table 1) was then normalized to clearly understand risk assessment by using following equation:

$$H_n = (H - H_{\min}) / (H_{\max} - H_{\min}) \quad (2)$$

where  $H_n$  is normalized value,  $H$  is total score of this site, and  $H_{\max}$  and  $H_{\min}$  are maximum and minimum score along this section of the highway.

#### 4.1.1 Kinematic analysis

Kinematic analysis is an important technique to know possible rockfall process based on joints and slope orientation. Field surveys were conducted to acquire joint data (orientation, spacing, aperture, filling, persistence) from rockfall sites. Then, kinematic analysis was carried out by using DIPS 7.0 software to interpret joint data to know their effect on slope and possible occurrence (Fig. 4). Most of the landslides including rockfalls took place on slope with angle more than  $30^\circ$  and was considered as friction angle in this area. Daylight envelop and friction cone were drawn to evaluate number of critical poles. Intersections between circle representing slope face and cone of friction are critical (Figs. 7a, 8c; Hoek and Bray 1981). Possibility of three possible failure modes (planer, toppling, wedging) has been assessed. In the end, whole information was supplemented with RHRS.

#### 4.2 Debris flow risk assessment

Risk is the product of hazard and anticipated damage to the exposed elements: property, lives, disruption of economic activity, etc. (= vulnerability  $\times$  amount; van Westen et al. 2006). In our case, vulnerability is highway's blockade, burial, erosion and traffic disruption directly affected by debris flows. All rating parameters were based on three main debris flow processes: initiation, transportation and deposition (Table 2). Rainfall water mobilizes debris downslope, and therefore, maximum rainfall for 24 h was considered for risk assessment. Stream steepness reflects its capacity to mobilize material downslope. It has been classified into three categories. Availability of debris and enough water supply in catchment area is a basic requirement for debris flow initiation. Quantity of collapsed material in terms of debris has a direct relation with magnitude and spreading of flow. Proportion of area covered by collapsed material (debris, scree, talus, moraines) to total

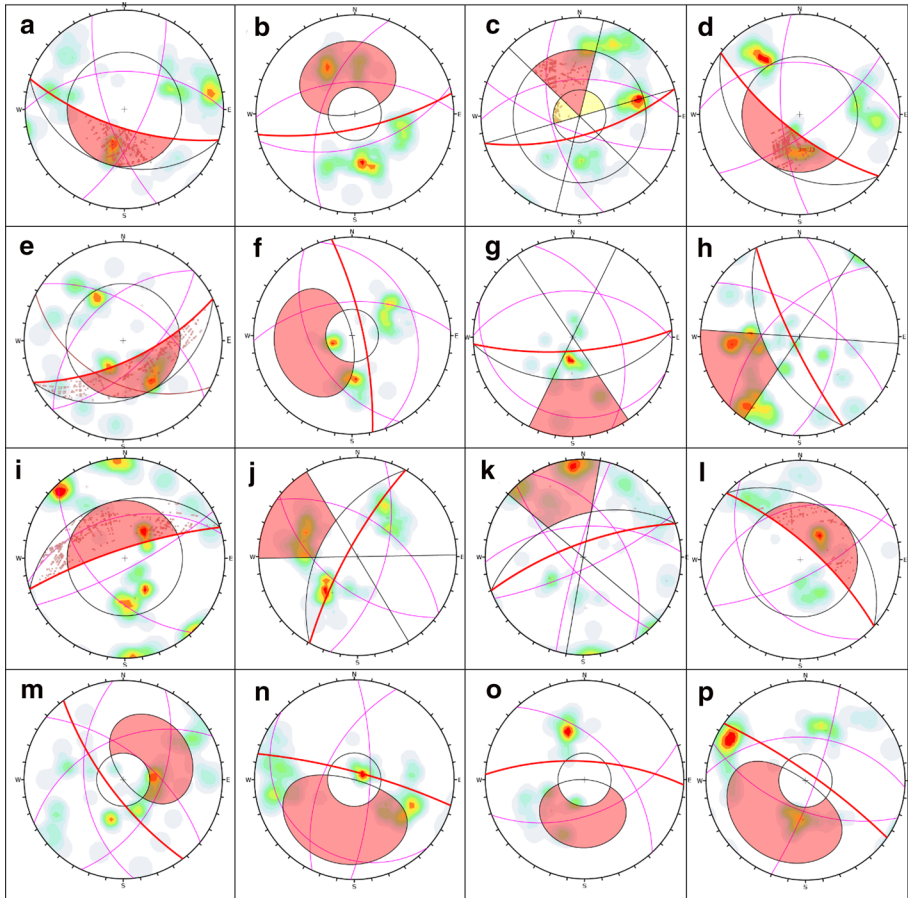


**Fig. 4** Kinematic analysis explaining major failure mode along some sites from the investigated rockfalls

catchment area has been calculated by satellite imagery. Furthermore, potential and recent slope failures were identified in catchment area to determine which can be source of debris flow.

Vegetation effects debris flow phenomenon by hindering or decelerating it. Therefore, its subjective evaluation was executed. Debris flow history, disaster mode and countermeasures to avoid disaster were taken into account for vulnerability assessment. Road clearance logs, field surveys and local community’s opinion were taken into account to know history of previous events. Rainfall water mobilizes debris downslope, and therefore, maximum rainfall for 24 h was considered for risk assessment. Stream steepness reflects its capacity to mobilize material downslope. It has been classified into three categories. Availability of debris and enough water supply in catchment area is a basic requirement for debris flow initiation. Quantity of collapsed material in terms of debris has a direct relation with magnitude and spreading of flow. Proportion of area covered by collapsed material (debris, scree, talus, moraines) to total catchment area has

**Table 2** Rating criteria for debris flows risk assessment

Parameters ▼	3 Points	9 Points	27 Points
<i>Hazard</i>			
24 h maximum rainfall (mm)	< 30	30–80	> 80
Maximum stream steepness	< 10°	10°–30°	> 30°
Area with slope gradient greater than 30° (km <sup>2</sup> )	< 0.08	0.08–0.20	> 0.20
Seepage	Dry	Dripping	Flowing
Slope failures in catchment area	No	Old scarps and potential failures	Active and potential failures
Area covered by vegetation	Thickly vegetated	Thinly vegetated	Sparsely vegetated/no vegetation
Rock mass characteristics	Massive rock mass	Banded rock mass	Sheared rock mass
Proportion of collapsed material to catchment area	< 0.1	0.1–0.3	> 0.3
<i>Vulnerability</i>			
Debris flow history	No past events	Past events without traffic disruption	Past events with traffic disruption
Countermeasures	Effective countermeasure	Ineffective countermeasures	No countermeasures
Potential disaster mode	Partial damage of bridge	Outflow of embankment	Debris flooding on road/damage of road

been calculated by satellite imagery. Furthermore, potential and recent slope failures were identified in catchment area to determine which can be source of debris flow.

## 5 Results

### 5.1 Analysis of landslide inventory

According to road clearance logs, mass movements interrupted traffic flow along this particular section (200 km) for two hundred and twenty-six (226) times at one hundred and four (104) locations during a period of 4 years (August 1996—July 2000; Fig. 5; Khan et al. 2003). The mass movements are mainly rockfalls (47), debris flows (26), debris slides (26) and historical deep-seated rockslides (5). Size of these landslides varies from minimum ninety square metres (shallow) to maximum ten square kilometres (deep seated). After interpretation of satellite imagery, previous publications and field surveys, rockfalls and debris flow along this section were major concern and investigated in this study. Due to uncontrolled blasting, the highly fragmented Jijal complex and massive amphibolites have a large number of rockfalls along cut slopes. The Pattan earthquake triggered many rockfalls leading to severe damage on these two locations. Near Kandia valley, short persistence stress release joints in massive diorite of Chilas complex led into formation of large blocks ( $> 6\text{m}^3$ ). It is sometimes impossible to remove these large blocks from the highway without blasting. Debris flows along Jijal-Pattan and Sazin-Chilas subsections are common (Fig. 6). However, the presence of active faults (MMT and Pattan fault) in former subsection made debris available and torrential rains in Monsoon transport it. Therefore, frequency of the debris flow and rockfall is quite high in the section (Fig. 5). However, the highway takes a sharp bend after Sazin and enters semi-arid to arid zone with low precipitation. Also, later section has sparsely vegetated relatively large catchment areas. Both these factors are responsible for low frequency of the slope failures (Fig. 5).

### 5.2 Risk analysis of rockfalls

Potential rockfall sites identified after landslide inventory analysis and runout assessment by empirical model Flow-R were surveyed in detail. Keeping in mind controlling parameters in our study area, modified Pierson's RHRS was applied (Table 1). Four rockfall sites (Jijal, Chochang, Lotar and Summar nala) are discussed as examples.

#### 5.2.1 Jijal rockfall

This rockfall is along a cut slope and active since construction of the highway. It is located in close vicinity of Jijal (Fig. 10a). Being part of hanging wall of MMT, it is highly jointed. Furthermore, excavation by uncontrolled blasting aggravated the situation. The Pattan and Muzaffarabad earthquake triggered rockfall leading to complete destruction during former event. This site had high peak ground acceleration (PGA) value (64.73%; USGS database 2019) during this event with intensity (MMI) of seven. Effective slope is 65 m high and comprised of pyroxenites and serpentinites. It is characterized by three joint sets with open apertures and an adverse impact on slope stability. Foliation has also been considered as a joint set. Joints are closely spaced leading to formation of block with maximum size  $> 0.25\text{m}^3$ . Rockfalls are frequent throughout the year, especially in Monsoon rainy season and at

the end of continuous freeze–thaw cycles. While travelling towards Besham, PDS is 13%, which is very low, whereas towards Chilas, it is more than 80%. Distance between highway and slope is less than 2 m, which is not enough to trap blocks falling down. Wedging was found major failure mode along with toppling. All these parameters and absence of protective measure have aggravated the situation. Calculated normalized value of this site was 0.98 and therefore was placed under very high-risk category.

### 5.2.2 Chochang rockfall

Overhangs produced by uncontrolled blasting with heavy explosives for road excavation characterize this section. Rockfall in these overhangs along this part of the highway is regular phenomenon during rains. In April 2016, rockfall damaged, buried highway and blocked traffic for a week at this particular location (Fig. 10c). Tectonized banded amphibolites constitute 148-m-high slope in this area. Three joint sets exist with open apertures, undulating joint planes, with clay filling and with an overall adverse impact on slope stability (Fig. 4f). Based on previous seismic events, seismic intensity was marked as VI at this site. Deposit of recent rockfall indicates variation in block size from few  $\text{cm}^3$  to  $2 \text{ m}^3$ . The absence of countermeasure and effective ditch along the highway makes it vulnerable. However, PDS is 100% from both direction of the highway decreasing vehicle's vulnerability. During kinematic analysis, toppling was found major mode of failure. Computed normalized value for this site was 0.74, placing it under high risk.

### 5.2.3 Lotar rockfall

The rockfall site is located near Dwyter Valley Bridge (Fig. 10c). This area marks the entry of the Kamila fault (KF) in valley. Slope is combination of both cut and natural slope, with effective height of 215 m. Gabbro-norites are primary slope component, which is jointed and sheared at different places. During discontinuity survey, three joints were found with one joint dipping along the slope, facilitating plane failure (Fig. 4h).

Joints are closely spaced with open apertures leading to formation of blocks  $< 0.06 \text{ m}^3$ . The site has seismic intensity of VI in previous earthquakes. Well-developed pile of failed mass at toe indicates frequency and history of rockfalls. Distance between highway and slope is less than 2 m, indicating low ditch effectiveness. Furthermore, while travelling towards Besham, PDS is quite low (26%). There is no protection for the road and travellers adding more to vulnerability. Overall, this zone was ranked at high risk with score of 0.71.

### 5.2.4 Yadgar rockfall

This site is located between Kandia valley bridge and Summer Nala ( $35.496822^\circ\text{N}$ ,  $73.298431^\circ\text{E}$ ) (Fig. 7a). Torrential rains in Monsoon and Westerlies trigger rockfalls every year. Strongly foliated, massive gabbro-norites and diorites constitute 411 m high slopes in this zone. During discontinuity survey, data related to 58 joints were collected. We found three joint sets with their mean dip direction/dip  $105/60$ ,  $218/54$  and  $070/50$ , respectively. In addition to these joints, stress release joints with short persistence were found. These short persistence stress release joints and large normal joint spacing led into formation of huge blocks of more size more than  $6 \text{ m}^3$  (Fig. 7). Removal and mobilization of these blocks without blasting is almost impossible. During kinematic analysis, both plane and

toppling were found prominent failure modes (Fig. 7). While travelling towards the Chilas, an impulsive turn before these sites limits decision distance, and therefore, PDS was found low (20%). All discussed parameters, ineffective ditch and lack of countermeasures turned this zone into very high-risk zone with normalized score of 1.

### 5.2.5 Pattan Bazar rockfall

The Pattan rockfall is located close to the Pattan fault, responsible for 1974 earthquake. It was identified as potential site during regional study. Detailed survey was conducted to rate all parameters (Table 1) for categorisation of the site. Massive gabbro and diorites characterize the slope along the highway. Three closely spaced joint sets (including foliation) control the stability of slope with wedging as a major failure process (Fig. 8). Moreover, foliation is dipping towards the highway. Effective height of the slope is 26 m, with occasional falls, scattered pile of failed mass and least ditch effectiveness (Fig. 8). DSD is 70%, enabling the traveller to make an instant decision beforehand. Overall, the site was placed in intermediate risk category with normalized score of 0.36.

## 5.3 Risk analysis of debris flows

Potential debris flow identified during first step was then rated using Table 2. Each parameter was cautiously evaluated. Afterwards, total score of each site was normalized and classified. Following two examples are explained to give an overview of the rating criteria (Fig. 9).

### 5.3.1 Serai debris flow

The site is located at 30 km from Besham towards Chilas ( $35^{\circ} 4'13.00''\text{N}$ ,  $72^{\circ}57'18.91''\text{E}$ ; Fig. 10a), in Monsoon region, receiving maximum daily rainfall more than 80 mm. Blockade of highway at this site due to torrential rainfall is common. In April 2017 and 2018, 30 m of the highway was completely buried under its deposits. The catchment area ( $1.20 \text{ km}^2$ ) is thinly vegetated, has 18% area with collapsed material produced by continuous slope failures in highly fragmented garnet pyroxenites. The channel is 1.59 km long with gradient of 1.23 km. Moreover, it is young and steep ( $> 40^{\circ}$ ) at places having a lot of debris. Both active and potential slope failures have been found in catchment area, which are possible source of upcoming debris flows. There was continuous water seepage in the channel. Previously, due to absence of efficient drain or effective countermeasures, debris flow was directly flooding over the highway. There is an embankment on opposite side, to avoid the highway's erosion, which is not enough to minimize damage. The calculated normalized score was 0.91 and ranked as very high-risk site.

### 5.3.2 Harbon Debris Flow

The Harbon site is located at  $35^{\circ}31'23.21''\text{N}$  and  $73^{\circ}39'36.03''\text{E}$ , 5 km east of Harbon Nala and in non-monsoon region with daily rainfall less than 45 mm (Fig. 11b). The site is a part of an historical large rockslide deposit ( $\sim 4 \text{ km}^3$ ), which dammed Indus River (age is unknown). Gully erosion is prominent in this deposit, and furthermore, all gullies converge to a single gully, with steepness more than  $30^{\circ}$  at places. The catchment area ( $6 \text{ km}^2$ ) is sparsely vegetated with high percentage of collapsed material (33%). Furthermore, slope

**Table 3** Percentage of different classes in final risk map

Risk level	Length (km)	Percentage of total length (%)
Very high	25.13	12.56
High	37.34	18.67
Intermediate	57	28.48
Low	80.56	40.28

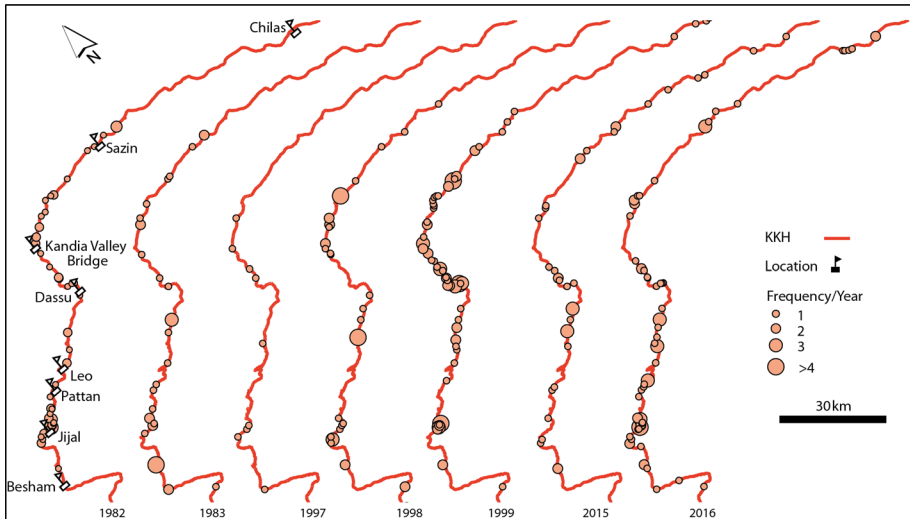


**Fig. 5** Landslide frequency map of the studied section, encompassing over 7 years

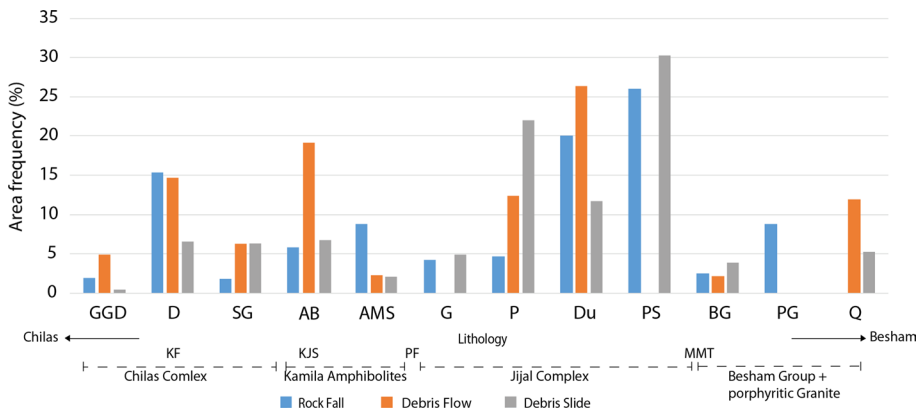


**Fig. 6** Area frequency of falls, slides and flows in lithologies, exposed along the studied section. For abbreviations, please see Fig. 1



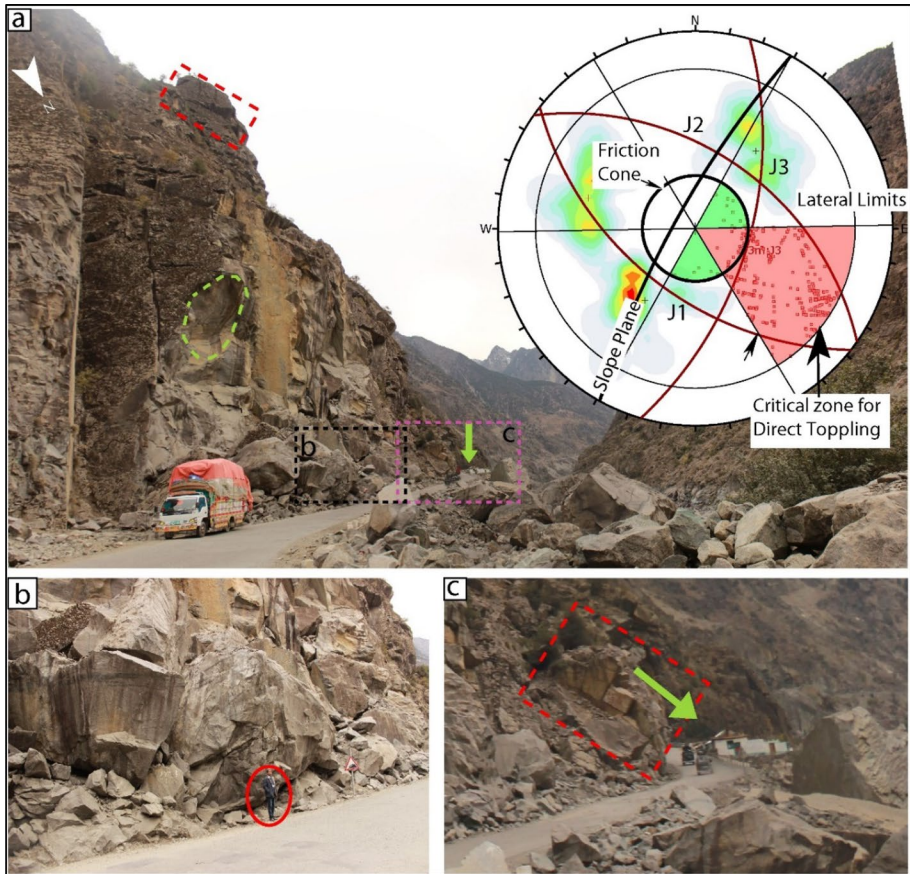


**Fig. 7** a An overview of Yadgar Rockfall (see location in 10a): it is a cutslope with an effective long natural slope (not visible). Large joint spacing and aperture has led into formation of huge blocks. Green circle is representing fresh scar. Red rectangle contains a loosely held block, which can be a possible failure. Deposit of failed rock mass is also visible. Green arrow is pointing towards highway’s turn just before site, decreasing driver’s decision sight distance. Pink and black rectangles show locations of (b) and (c). Stereographic projections explain orientation of joints, slope and major possible failure mode as direct toppling. b Size of block > 6m<sup>3</sup> (Scale: man in red circle). c Planer failure in loosely held blocks

failures in scarp and in deposit of old landslide are providing debris material. In April 2016, heavy rain initiated debris flow, which flooded, buried and blocked the highway for traffic. The absence of culvert, bridge and other effective measure placed this site at very high risk with normalized risk score of 0.82.

### 5.3.3 Risk map

It was an impossible task to assess debris flow and rockfall risk along entire 200 km stretch of the highway, by surveying each site in detail. Therefore, potential hazardous sites were identified by using regional approach, which were further investigated in detail during field surveys. Rockfalls (47) and debris flows (26) were rated by using Tables 1 and 2. Score of

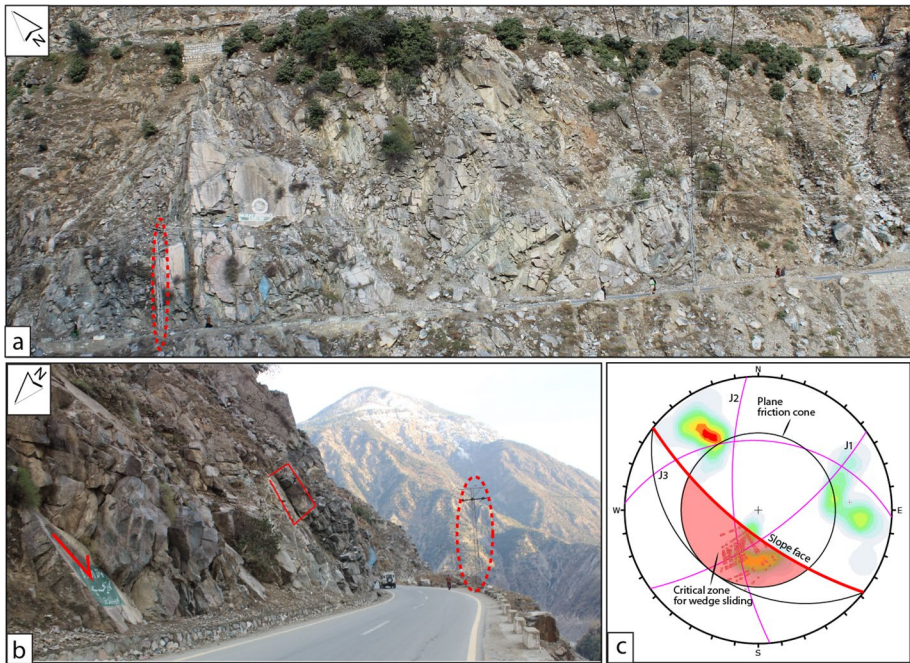


**Fig. 8** **a** An overview of Pattan Bazar rockfall. Red ellipse shows a pole (9 m high) as a scale. **b** Another view of the site, explaining structural control, ditch effectiveness and DSD. **c** Kinematic analysis of wedge sliding as main failure mode

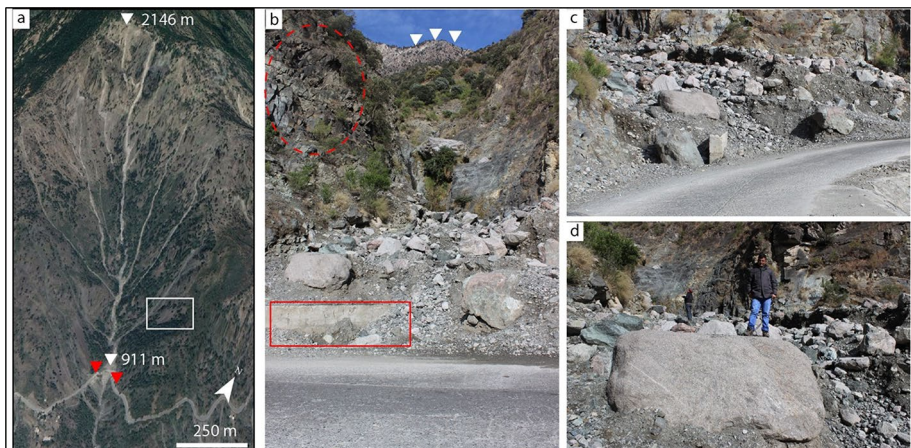


**Fig. 9** **a** Overview of Serai debris flow: source area of the catchment ( $1.20 \text{ km}^2$ ) is sparsely vegetated, having vertical gradient of 1.23 km over 1.59 km (Google Earth 2017). White rectangle shows a slope failure within catchment area. Red arrows mark the highway. **b** Red rectangle represents poorly designed silt wall over drain, now completely blocked by deposit. Red circle shows highly fragmented rock mass, which is almost same throughout the catchment. White arrows represent the highest part of the catchment. **c** Side view of cause way and debris flooding the highway directly. **d** Variety of grain sizes, from silt to large boulder ( $> 2 \text{ m}^3$ )

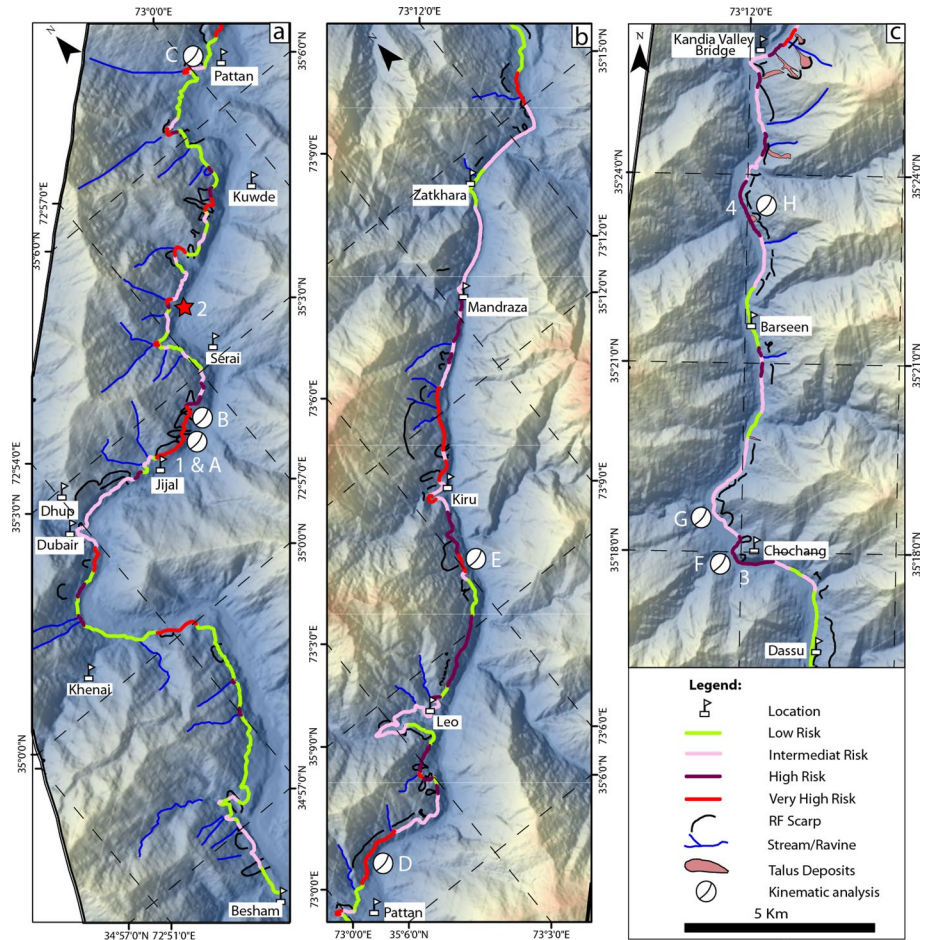


**Fig. 10** Risk map of the studied section, **a** Besham-Pattan, **b** Pattan–Dassu, **c** Dassu–Kandia Valley. Numbers in white colours show location of explained examples: 1—Jijal Rockfall, 2—Serai Debris Flow, 3—Chochang Rockfall, 4—Lotar Rockfall, 5—Pattan Bazar Rockfall. Red star gives location of Fig. 6 and 8. Whereas, white circles are showing the location of Fig. 4

each site was normalized by using Eq. 2, further classified into four classes by equal interval technique: low, intermediate, high and very risk (Figs. 10, 11). Very high and high risk were found along 12.56% and 18.67% of the section, respectively, whereas 61% of this section accounts for low and intermediate risk (Table 3).

Breakup of rockfall sites against scoring category and parameters indicates that the absence of effective countermeasures, DSD and failed mass at toe were responsible for placement of the most of sites in very high-risk category. However, almost 60% sites have an effective slope height with maximum score (Table 4).

The highway near Jijal, Pattan, Kiru, Chochang, Lotar, Samar Nala and Kandian was at very high risk. Active faults (MMT, PF and KF) and shear zones in these parts degraded rock mass where differential erosion triggered rockfall during heavy rain and seismicity.

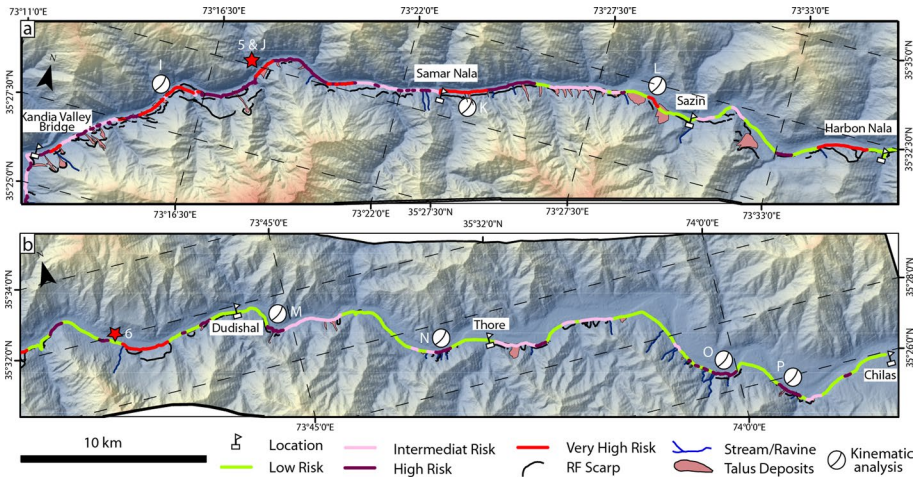


**Fig. 11** Risk map of the studied section, **a** Kandia Valley-Harbon Nala, **b** Harbon Nala-Chilas. Numbers in white colour show location of explained examples: 5—Yadgar Rockfall, 6—Harbon Debris Flow. Red star gives location of Fig. 7. Whereas, white circles are showing the location of Fig. 4

**Table 4** Percentages of rockfall sites in each scoring category against each parameter

Parameter ▼	Scoring category ►			
	3 Points	9 Points	27 Points	81 Points
Slope height (m)	2	11.8	26.5	59.7
Number of joint sets and their effect on slope	11.54	19.23	38.46	30.77
Joint spacing (m)	5.9	64.7	17.6	11.8
Joint planes	10.5	26.3	47.4	15.8
Seismic intensity	0.0	35.3	29.4	29.4
Block size (m <sup>3</sup> )	42.1	10.5	21.1	26.3
Rockfall history	5.9	17.6	47.1	29.4
Failed mass at toe	5.3	10.5	36.8	47.4
DSD	31.6	10.5	5.3	52.6
Ditch effectiveness	5.3	15.8	5.3	73.7
Protection measures	6.7	3.1	10.0	80.2

The subsection between Jijal and Sazin is characterized by steep topography, having rockfall a major concern, whereas section between Sazin and Chilas passes through broad valley except few places after Harbon Nala. Mostly, it lies at low to intermediate risk except some locations. In past, sparsely vegetated, large catchment areas with enough debris supply generated hazardous debris flows in this area. Overall absence

of countermeasures is a serious threat to highway's stability. Construction of effective countermeasures can change or minimize risk level of all sites.

## 6 Discussion and conclusion

In this study, regional to site-specific approach (quantitative to semi-quantitative) was used to prepare risk map along a section of the KKH. In first phase, remote sensing was used to find potential hotspots, required to be investigated in detail. Source areas were defined by using two different techniques. DEM-based slope angle distribution (SAD) was used to identify rockfall source areas. High-resolution DEM has ability to detect even smaller source areas (Michoud et al. 2012) and has an ultimate impact on quality of results. Therefore, DEM with 12 m resolution was used for most of the area. The presence of no-data values in 12 m DEM has forced us to use low resolution (30 m) for some areas. For debris flows, predefined mapped sources were used for runout assessment. Flow-R was employed to assess approximate extent and impact of debris flows and rockfalls on the highway.

Basic advantage of this software is that it can work with limited data and customized options, which allowed us to modify it according to local conditions. However, it had also some limitations, as it did not account some local parameters (weathering, structural conditions, etc.) and volume but only surface area. Propagation extent of flows and falls was marginally more than real events, which decreased possibility of exclusion of even single observed event. Potential sites identified during this process were then surveyed in detail. Keeping in view nature of slope failures, two different rating criteria were used for risk assessment.

Modified Pierson's RHRS was used to assess risk related with rockfalls. Eleven parameters grouped in four categories were considered for rating (Table 1). Evaluation of some parameters was subjective, depending upon expert judgement. RHRS is flexible and can be modified according to local geomorphological, geological and climatic conditions. PSD was carefully calculated and highway authorities cleared confusion created by the absence of speed limit posters along some parts of the KKH. Due to insufficient daily data regarding vehicles passing through section, average vehicle risk (AVR) was not taken into account. Width of the highway in this section is constant and therefore has not been considered. Kinematic analysis showed toppling and wedging major rockfall process along the studied section. Risk assessment of debris flow was executed by using semi-quantitative technique. Keeping in mind, basic components of debris flow (formation, initiation, transportation and deposition), eleven parameters were opted (Table 2).

Rainfall intensity is not uniform along studied section; therefore, daily maximum rainfall was included. Three parameters in both rating criteria were about current state of countermeasures and their capacity to protect highway and traveller from hazard. Change in their current status can lead to decrease or increase vulnerability of the highway. Sum of scores of all parameters was then normalized using Eq. 2. It is pertinent to mention that scores of rockfalls and debris flows were normalized separately. Equal interval classification method was applied to categorize the final risk map into four: very high, high, intermediate and low risk. Sites near Jijal, Kiru, Chochang, Yadgar, Kandian valley and Harbon Nala were found at very high risk. Section between Besham and Dubair, Dudishal and Chilas were safer with low to intermediate risk except a few sites with high score. Highway authorities can plan curative work according to risk level calculated. Sites with very high risk require immediate inspection and countermeasures. Otherwise, highway can

potentially be blocked for more than 2 days at these sites. Highway section with high risk has capacity to block traffic for less than a day. Warning signs and regular inspection are obligatory for these sites. Intermediate risk means no blockade but can damage vehicle or traveller. Low risk areas are quite safe and require no countermeasures. Methods and techniques applied in this study can further be used for prioritization of road and highways affected by rockfalls and debris flows.

**Acknowledgements** We would like to thank Higher Education Commission (HEC) of Pakistan and German Academic Exchange Service (DAAD) for financial support for the research project, Prof Dr Florian Amann, Dr Anja Dufresne, Dr Muhammad Shafique, Mr. Yasir Sarfraz and Mr. Aram Fathian Baneh for their support and valuable suggestions. Further, we would like to acknowledge Frontier Works Organization (FWO), National Highway Authority (NHA) and Japan International Cooperation Agency (JICA) Islamabad for their support.

**Funding** Open Access funding enabled and organized by Projekt DEAL..

**Open Access** This article is licensed under a Creative Commons Attribution 4.0 International License, which permits use, sharing, adaptation, distribution and reproduction in any medium or format, as long as you give appropriate credit to the original author(s) and the source, provide a link to the Creative Commons licence, and indicate if changes were made. The images or other third party material in this article are included in the article's Creative Commons licence, unless indicated otherwise in a credit line to the material. If material is not included in the article's Creative Commons licence and your intended use is not permitted by statutory regulation or exceeds the permitted use, you will need to obtain permission directly from the copyright holder. To view a copy of this licence, visit <http://creativecommons.org/licenses/by/4.0/>.

## References

- Ahmed MF, Rogers JD, Ismail EH (2014) A regional level preliminary landslide susceptibility study of the upper Indus river basin. *Eur J Remote Sens* 47:343–373. <https://doi.org/10.5721/EuJRS20144721>
- Ali S, Biermanns P, Haider R, Reicherter K (2018a) Landslide susceptibility mapping by using GIS along the China Pakistan economic corridor (Karakoram Highway), Pakistan. *Nat Hazards Earth Syst Sci*. <https://doi.org/10.5194/nhess-2018-39>
- Ali S, Tayyib Riaz M, Yasir Sarfraz, et al (2018b) Rock fall and debris flow hazard and risk assessment along Karakoram Highway (Besham-Chilas Section). In: EGU general assembly 2018
- Ambraseys N, Lensen G, Moinfar A, Penningtons W (1981) The Pattan (Pakistan) earthquake of 28 December 1974: field observations. The earliest known earthquakes of the Northwest Frontier. Provinces (NWFP) Geological and tectonic setting Evidence of regional Quaternary and Recent movements. *Q J Eng Geol Hydrogeol* 14:1–16
- Bacha AS, Shafique M, van der Werff H (2018) Landslide inventory and susceptibility modelling using geospatial tools, in Hunza-Nagar valley, northern Pakistan. *J Mt Sci* 15:1354–1370. <https://doi.org/10.1007/s11629-017-4697-0>
- Basharat M, Shah HR, Hameed N (2016) Landslide susceptibility mapping using GIS and weighted overlay method: a case study from NW Himalayas, Pakistan. *Arab J Geosci* 9:1–19. <https://doi.org/10.1007/s12517-016-2308-y>
- Baumann V, Wick E, Horton P, Jaboyedoff M (2010) Debris flow susceptibility mapping at a regional scale along the National Road N7, Argentina. In: Proceedings of the 14th Pan-American conference on soil mechanics and geotechnical engineering
- Budetta P (2004) Assessment of rockfall risk along roads. *Nat Hazards Earth Syst Sci* 4:71–81. <https://doi.org/10.5194/nhess-4-71-2004>
- Budetta P, De Luca C, Nappi M (2016) Quantitative rockfall risk assessment for an important road by means of the rockfall risk management (RO.MA.) method. *Bull Eng Geol Environ* 75:1377–1397. <https://doi.org/10.1007/s10064-015-0798-6>
- Cao C, Xu P, Chen J et al (2016) Hazard assessment of debris-flow along the Baicha River in Heshigten Banner, Inner Mongolia, China. *Int J Environ Res Public Health* 14:30. <https://doi.org/10.3390/ijerph141010030>

- Capra L, Macías JL, Scott KM et al (2002) Debris avalanches and debris flows transformed from collapses in the Trans-Mexican Volcanic Belt, Mexico: behavior, and implications for hazard assessment. *J Volcanol Geotherm Res* 113:81–110. [https://doi.org/10.1016/S0377-0273\(01\)00252-9](https://doi.org/10.1016/S0377-0273(01)00252-9)
- Chen HX, Zhang LM, Chang DS, Zhang S (2012) Mechanisms and runout characteristics of the rainfall-triggered debris flow in Xiaojiagou in Sichuan Province, China. *Nat Hazards* 62:1037–1057. <https://doi.org/10.1007/s11069-012-0133-5>
- Cui P, Xiang LZ, Zou Q (2013) Risk assessment of highways affected by debris flows in Wenchuan earthquake area. *J Mt Sci* 10:173–189. <https://doi.org/10.1007/s11629-013-2575-y>
- Derbyshire E, Fort M, Owen LA (2001) Geomorphological hazards along the Karakoram Highway: Khunjerab Pass to the Gilgit River, northernmost Pakistan. *Erdkunde* 55:49–71. <https://doi.org/10.3112/erdkunde.2001.01.04>
- Fairfield J, Laymarie P (1991) Drainage networks from grid digital elevation models. *Water Resour Res* 30(6):1681–1692
- Fayaz A, Latif M, Khan KSA (1985) Landslide evaluation and stabilization between Gilgit and Thakot along the Karakoram Highway. Geological Survey of Pakistan, Islamabad
- Ferlisi S, Cascini L, Corominas J, Matano F (2012) Rockfall risk assessment to persons travelling in vehicles along a road: the case study of the Amalfi coastal road (southern Italy). *Nat Hazards* 62:691–721. <https://doi.org/10.1007/s11069-012-0102-z>
- Gentile F, Bisantino T, Trisorio Liuzzi G (2008) Debris-flow risk analysis in south Gargano watersheds (Southern-Italy). *Nat Hazards* 44:1–17. <https://doi.org/10.1007/s11069-007-9139-9>
- Guzzetti F, Reichenbach P, Wieczorek GF (2010) Rockfall hazard and risk assessment in the Yosemite Valley, California, USA. *Nat Hazards Earth Syst Sci* 3:491–503. <https://doi.org/10.5194/nhess-3-491-2003>
- Hewitt K (2001) Catastrophic rockslides and the geomorphology of the Hunza and Gilgit River Valleys, Karakoram Himalaya. *Erdkunde* 55:72–93. <https://doi.org/10.3112/erdkunde.2001.01.05>
- Hewitt K (1998) Catastrophic landslides and their effects on the Upper Indus streams, Karakoram Himalaya, northern Pakistan. *Geomorphology* 26:47–80. [https://doi.org/10.1016/S0169-555X\(98\)00051-8](https://doi.org/10.1016/S0169-555X(98)00051-8)
- Hewitt K, Gosse J, Clague JJ (2011) Rock avalanches and the pace of late quaternary development of river valleys in the Karakoram Himalaya. *Bull Geol Soc Am* 123:1836–1850. <https://doi.org/10.1130/B30341.1>
- Hoek E, Bray J (1981) *Rock slope engineering*, 3rd edn. Institution of Mining and Metallurgy, London
- Holmgren P (1994) Multiple flow direction algorithms for runoff modelling in grid based elevation model. *Hydrol Process* 8(4):327–334
- Horton P, Jaboyedoff M, Zimmermann M, Mazotti B, Longchamp C (2011) Flow-R, a model for debris flow susceptibility mapping at a regional scale - some case studies. In: Proceedings of the 5th international conference on debris-flow hazards "mitigation, mechanics, prediction and assessment": Italian Journal of Engineering Geology, pp 875–884. doi: <https://doi.org/10.4408/IJEGE.2011-03.B-095>
- Hürlimann M, Copons R, Altimir J (2006) Detailed debris flow hazard assessment in Andorra: a multidisciplinary approach. *Geomorphology* 78:359–372. <https://doi.org/10.1016/j.geomorph.2006.02.003>
- Jaboyedoff M, Labiouse V (2003) Preliminary assessment of rockfall hazard based on GIS data. In: ISRM 2003 – Technology Roadmap for Rock Mechanics, pp 575–578
- Jaboyedoff M, Rudaz B, Horton P (2011) Concepts and parameterization of Perla and FLM model using Flow-R for debris flow. In: Proceedings of the 5th Canadian conference on geotechnique and natural hazards, vol 14, p 11414
- Kamp U, Growley BJ, Khattak GA, Owen LA (2008) GIS-based landslide susceptibility mapping for the 2005 Kashmir earthquake region. *Geomorphology* 101:631–642. <https://doi.org/10.1016/j.geomorph.2008.03.003>
- Kanwal S, Atif S, Shafiq M (2016) GIS based landslide susceptibility mapping of northern areas of Pakistan, a case study of Shigar and Shyok Basins. *Geomat Nat Hazards Risk* 5705:1–19. <https://doi.org/10.1080/19475705.2016.1220023>
- Khan H, Shafique M, Khan MA et al (2018) Landslide susceptibility assessment using frequency ratio, a case study of northern Pakistan. *Egypt J Remote Sens Sp Sci* 22:11–24. <https://doi.org/10.1016/j.ejrs.2018.03.004>
- Khan KSA, Fayaz A, Hussain M, Latif M (2003) *Landslides problems and their mitigation along the Karakoram Highway*, 1st edn. Geological Survey of Pakistan, Islamabad
- Khan KSA, Fayaz A, Latif M, Wazir AK (1986) *Rock and Debris slides between Khunjerab pass and Gilgit along the Karakoram Highway*. Geological Survey of Pakistan, Islamabad
- Kibria S, Masud B (2006) Tackling landslides during extension of KKH. In: Pakistan engineering congress, 70th annual session proceedings, pp 264–292

- Lari S, Frattini P, Crosta G, et al (2011) Rockfall and debris flow societal and economic risk assessment at the regional scale. In: Acts 10th World Water Day, Accad Naz dei Lincei - Atti dei Convegni Lincei, pp 179–187
- Liang WJ, Zhuang DF, Jiang D et al (2012) Assessment of debris flow hazards using a Bayesian network. *Geomorphology* 171–172:94–100. <https://doi.org/10.1016/j.geomorph.2012.05.008>
- Liu K-F, Li H-C, Hsu Y-C (2009) Debris flow hazard assessment with numerical simulation. *Nat Hazards* 49:137–161. <https://doi.org/10.1007/s11069-008-9285-8>
- Losasso L, Derron MH, Horton P et al (2016) Definition and mapping of potential rockfall source and propagation areas at a regional scale in Basilicata region (Southern Italy). *Rend Online Soc Geol Ital* 41:175–178. <https://doi.org/10.3301/ROL.2016.122>
- Loye A, Jaboyedoff M, Pedrazzini A (2009) Identification of potential rockfall source areas at a regional scale using a DEM-based geomorphometric analysis, pp 1643–1653
- Ma C, Hu K, Tian M (2013) Comparison of debris-flow volume and activity under different formation conditions. *Nat Hazards* 67:261–273. <https://doi.org/10.1007/s11069-013-0557-6>
- Michoud C, Derron MH, Horton P et al (2012) Rockfall hazard and risk assessments along roads at a regional scale: example in Swiss Alps. *Nat Hazards Earth Syst Sci* 12:615–629. <https://doi.org/10.5194/nhess-12-615-2012>
- Mineo S, Pappalardo G, D'Urso A, Calcaterra D (2017) Event tree analysis for rockfall risk assessment along a strategic mountainous transportation route. *Environ Earth Sci*. <https://doi.org/10.1007/s12665-017-6958-1>
- Mineo S, Pappalardo G, Mangiameli M et al (2018) Rockfall analysis for preliminary hazard assessment of the cliff of taormina Saracen Castle (Sicily). *Sustainability* 10:1–18. <https://doi.org/10.3390/su10020417>
- Oppikofer T, Hermanns RL, Horton P et al (2014) Consequence assessment of large rock slope failures in Norway. *Geophys Res Abstr* 16:11286. <https://doi.org/10.13140/RG.2.2.12340.55682>
- Peila D, Guardini C (2008) Use of the event tree to assess the risk reduction obtained from rockfall protection devices. *Nat Hazards Earth Syst Sci* 8:1441–1450. <https://doi.org/10.5194/nhess-8-1441-2008>
- Petley D (2016) Landslide damage to the Karakoram Highway. In: *Voice Earth Sp. Sci. Community*. <https://blogs.agu.org/landslideblog/2016/04/13/karakoram-highway-1/>. Accessed 12 Jun 2018
- Pierson L, Davis S, Van VR (1993) Rockfall hazard rating system. Federal Highway Administration, Washington, D.C.
- Pritchard M, Porter M, Savigny W, et al (2005) CN rockfall hazard risk management system: experience, enhancements, and future direction. In: International conference on landslide risk management, 18th annual vancouver geotechnical society symposium, p 14
- Rahim I, Ali SM, Aslam M (2018) GIS based landslide susceptibility mapping with application of analytical hierarchy process in District Ghizer, Gilgit Baltistan Pakistan. *J Geosci Environ Prot* 06:34–49. <https://doi.org/10.4236/gep.2018.62003>
- Regmi AD, Cui P, Dhital MR, Zou Q (2016) Rock fall hazard and risk assessment along Araniko Highway, Central Nepal Himalaya. *Environ Earth Sci* 75:1–20. <https://doi.org/10.1007/s12665-016-5905-x>
- Rickenmann D (2016) Debris-flow hazard assessment and methods applied in engineering practice. *Int J Eros Control Eng* 9:80–90. <https://doi.org/10.13101/ijece.9.80>
- Santi PM, Hewitt K, VanDine DF, Cruz EB (2011) Debris-flow impact, vulnerability, and response. *Nat Hazards* 56:371–402. <https://doi.org/10.1007/s11069-010-9576-8>
- Sletten K, Stalsberg K, Rubensdotter L (2015) DEbris slides and debris flows. In: Geological Survey of Norway. <https://www.ngu.no/en/topic/debris-slides-and-debris-flows>. Accessed 10 Nov 2018
- Tarboton DG (1997) A new method for the determination of flow directions and upslope areas in grid digital elevation models. *Water Resour Res* 33(2):309–319
- Toppe R (1987) Terrain models: a tool for natural hazard mapping. *Proc Davos Symp Sept 1986*:629–638
- van Westen CJ, van Asch TWJ, Soeters R (2006) Landslide hazard and risk zonation: why is it still so difficult? *Bull Eng Geol Environ* 65:167–184. <https://doi.org/10.1007/s10064-005-0023-0>
- Varnes DJ (1978) Slope movement types and processes. In: Schuster RL, Krizek RJ (eds) *Landslides: analysis and control*. Transportation Research Board, National Academy of Sciences, Washington, DC
- de Wrachien D, Mambretti S (2011) Assessment of debris flow magnitude in small catchments of the lombardy alps: the val gola case study. *Agric Sci* 02:9–15. <https://doi.org/10.4236/as.2011.21002>